

Biomarkers for Breast Cancer Detection in the Resting-State Dynamics of the Hemoglobin Signal



Harry L. Graber¹, Rabah Al abdi², Yong Xu¹, and Randall L. Barbour^{1,3}

¹NIRx Medical Technologies LLC, 7083 Hollywood Blvd., Los Angeles CA 90028, USA

²Jordan University of Science and Technology, Irbid 22110, Jordan

³SUNY Downstate Medical Center, 450 Clarkson Ave, Brooklyn NY 11203, USA

Abstract:

Biomarkers that are promising for breast-cancer diagnosis are identified in resting-state dynamic measures of the vascular bed. The markers also encompass a large fraction of the breast volume, which shows little dependence on tumor size.

Introduction:

Evidence of increased tissue stiffness, presence of structural malformations, and altered perfusion of the vascular bed are known phenotypic markers for the presence of breast cancer [1,2]. Increased awareness of these phenomena has motivated our development of techniques that explore the naturally occurring dynamics of the hemoglobin signal that accompany modulation of the vascular tree and its interactions with tissue. In particular, our group has developed several different instrumentation platforms that are suitable for exploring tissue dynamics while a simultaneous bilateral exam is performed.

In one form, and following the spirit of a clinical breast exam, our system design combines optical measures with tactile sensing and controlled articulations [3]. However, the dimensionality of the information space that could be explored in pursuit of identifying suitable biomarkers has prompted us to also consider more limited data-collection conditions. One such consideration is a simple resting-state measure, wherein time-series optical measures are obtained from both breasts simultaneously under defined conditions of optode contact. Our initial aim was to compare such baseline measures to responses evoked by controlled provocations, with the expectation that findings of interest would align mainly with the latter. However, as evidenced by the findings reported here, promising findings have been obtained based solely on examination of the resting-state responses.

Methods:

Measurement data considered here were obtained during an fNIRS-based breast imaging study that was conducted primarily to evaluate the potential of applied-pressure maneuvers to enhance discovery and characterization of breast tumors ("Phenotype-Motivated Strategies for Optical Detection of Breast Cancer," this conference). After research participants gave informed consent and provided a brief medical history (see Table 1 for subject demographics), they were seated and the sensing heads (see Figure 1) were adjusted to make good contact with both breasts. The onset of the first pressure maneuver was preceded by a five-minute resting baseline scan.

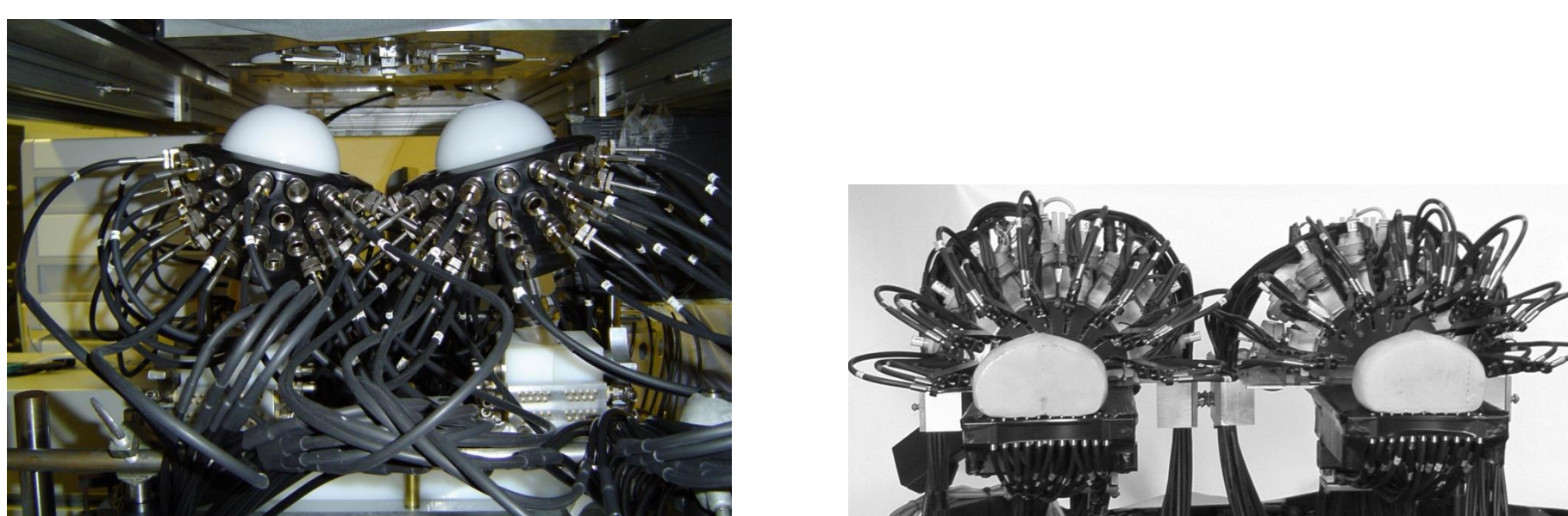


Figure 1. Photographs of the simultaneous dual-breast measuring heads, with phantoms in place, for the 1st-generation (left) and 2nd-generation (right) imagers.

Optical data were analyzed offline: application of a high-pass filter with a 0.01-Hz cutoff frequency was followed by use of the Normalized Difference Method to reconstruct images of oxygenated and deoxygenated hemoglobin (HbO₂, HbD), tissue oxygen saturation (HbSat), and blood volume (HbT) [4]. The resulting image time series (4D) were subsequently reduced to a set of five scalar metrics by: first, computing the temporal standard deviation (TSD) in each image voxel (4D → 3D) or the spatial mean (SM) or standard deviation (SSD) for each image time frame (4D → 1D); second, by computing the spatial mean and standard deviation of TSD (SMTSD, SSDTSD), temporal mean of SSD (TMSSD), and temporal standard deviation of SM and SSD (TSDSM, TSDSSD). With the same goal of probing different modulatory elements, we also have examined three additional quantities (CVSSD, CVTSD, SCI), each of which is a ratio of two metrics from the initial group of five.

$$SM(t) = \frac{\sum_r x(r,t)}{N_r}, \quad SSD(t) = \sqrt{\frac{\sum_r [x(r,t) - SM(t)]^2}{N_r}}, \quad TSD(r) = \sqrt{\frac{\sum_t x(r,t)^2}{N_t}}$$

$$SMTSD = \frac{\sum_r TSD(r)}{N_r}, \quad SSDTSD = \sqrt{\frac{\sum_r [TSD(r) - SMTSD]^2}{N_r}}$$

$$TMSSD = \frac{\sum_t SSD(t)}{N_t}, \quad TSDSSD = \sqrt{\frac{\sum_t [SSD(t) - TMSSD]^2}{N_t}}$$

$$TSDSM = \sqrt{\frac{\sum_t [SM(t)]^2}{N_t}}$$

$$CVSSD = 100 \frac{TSDSSD}{TMSSD}, \quad CVTSD = 100 \frac{SSDTSD}{SMTSD},$$

$$SCI = \frac{SMTSD}{TSDSM}$$

Device	Group-Level Parameter	Active Breast Cancer		Benign Breast Pathology	No Breast Pathology
		Left	Right		
1 st -Generation Imager	N	11	17	19	19
	Age [yr, mean (SD)]	47.5 (12.3)	51 (11.9)	45.6 (7.6)	43.3 (9.1)
	Tumor Size [cm, min-max (mean)]	0.8-7 (4.1)	0.8-11 (3.9)	n/a	n/a
2 nd -Generation Imager	N	12	6	23	22
	Age	53.9 (9.5)	53.7 (14.1)	48.1 (10.7)	51.5 (11.7)
	Tumor Size	0.5-6 (2.8)	1-5 (2.7)	n/a	n/a

Table 1. Subject-group descriptive information. Breast-cancer subjects include cases of invasive ductal carcinoma, invasive mucinous carcinoma, invasive lobular carcinoma, and 'occult' breast carcinoma [5].

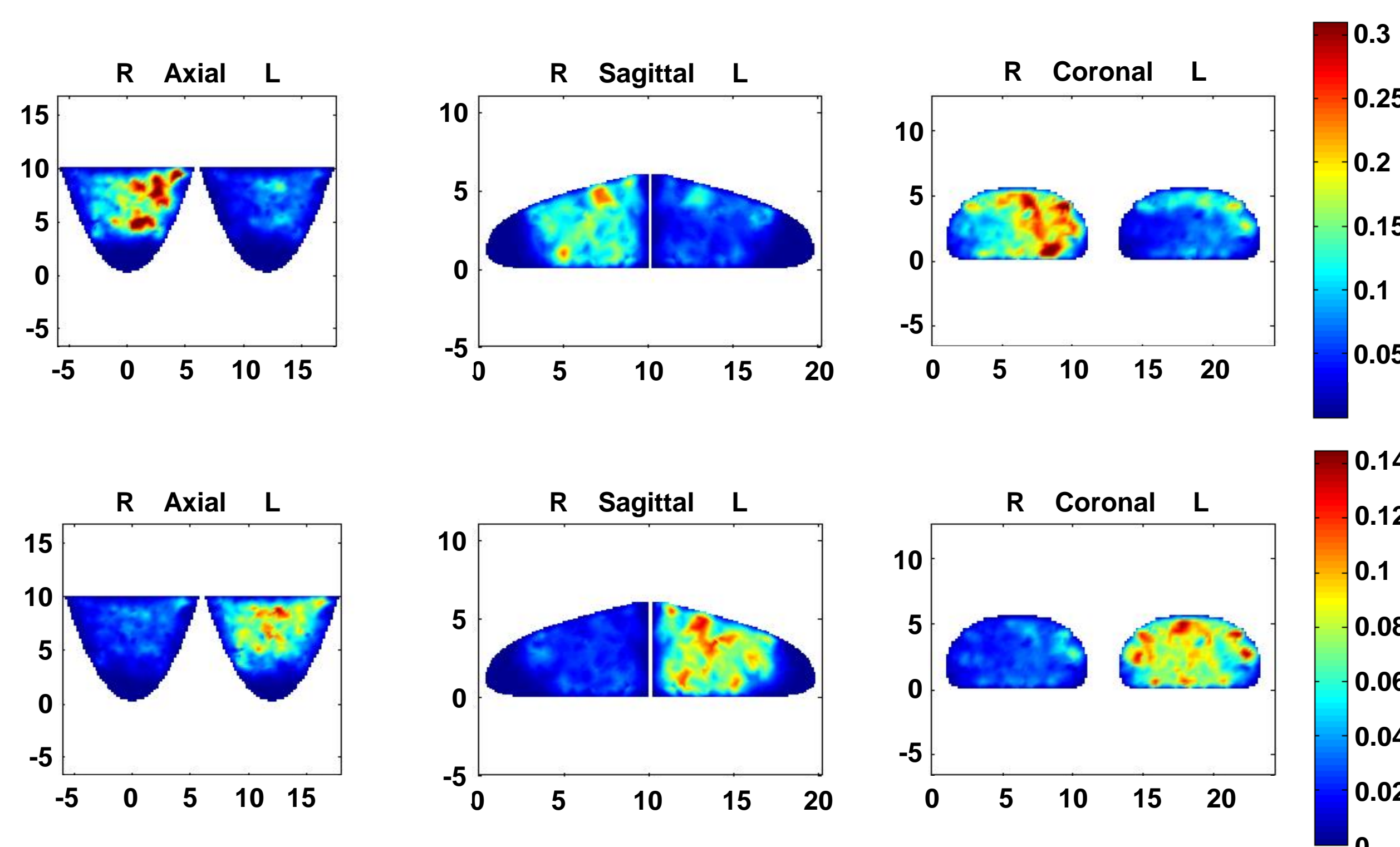


Figure 2. TSD spatial maps for representative breast-cancer subjects. (Top) Right-breast tumor (Grade-2 IDC, ER+), 1 cm, 4 o'clock; HbSat; 2nd generation; subject is 34 yo, BMI 29, size D. (Bottom) Left-breast tumor (Grade-3 IDC, ER+), 4 cm, 1 o'clock, HbSat; 2nd generation; subject is 50 yo, BMI 44, size C.

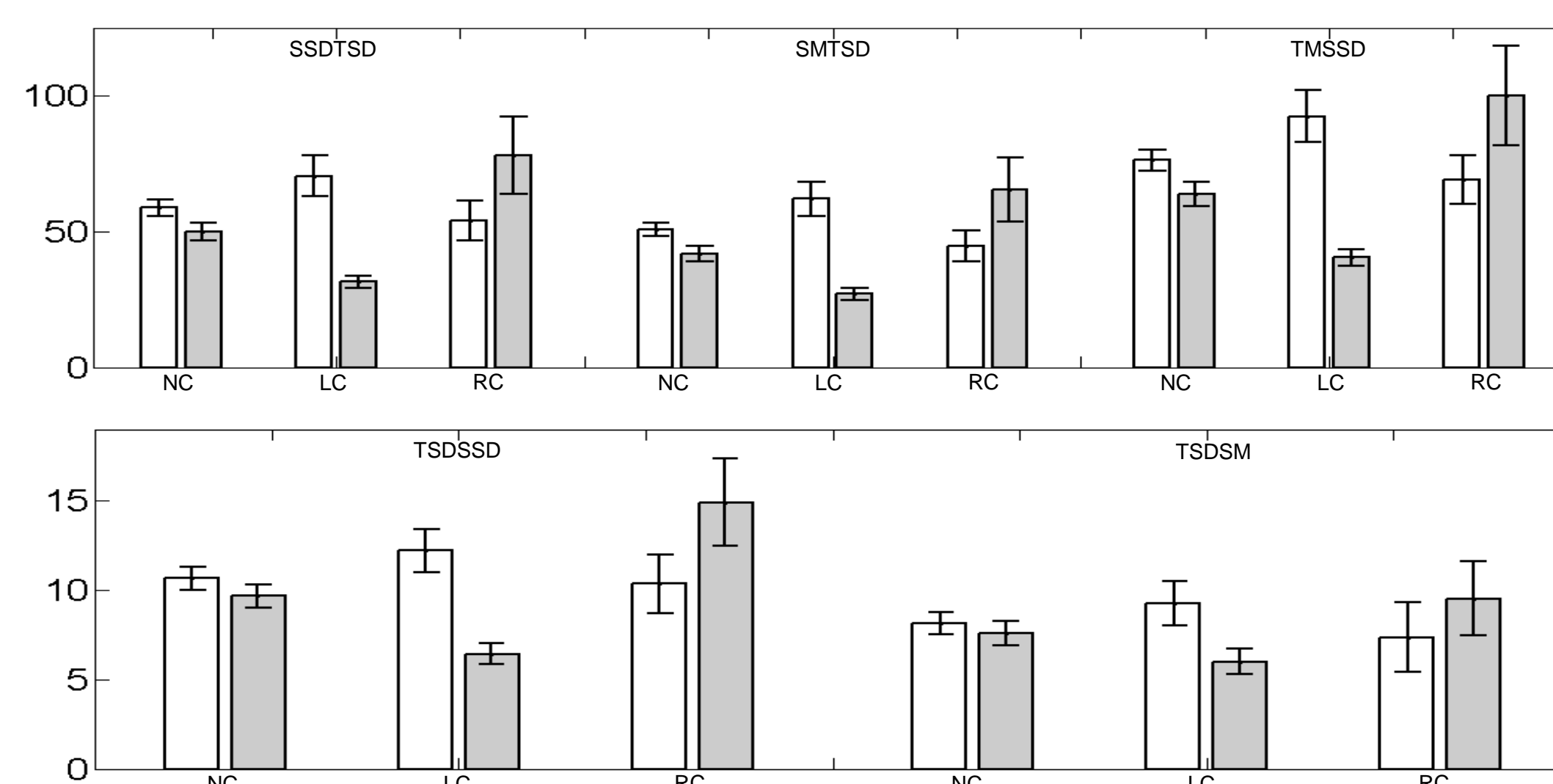


Figure 3. Unilateral group means (error bars = ±1 SEM) for the scalar metrics computed from HbSat image time series, for both the left (white bars) and right (gray bars) breast, for the non-cancer (NC), left-breast cancer (LC) and right-breast cancer (RC) subject groups. The largest single-breast group mean overall was arbitrarily set to 100, and all other group means and all SEMs were rescaled to that unit.

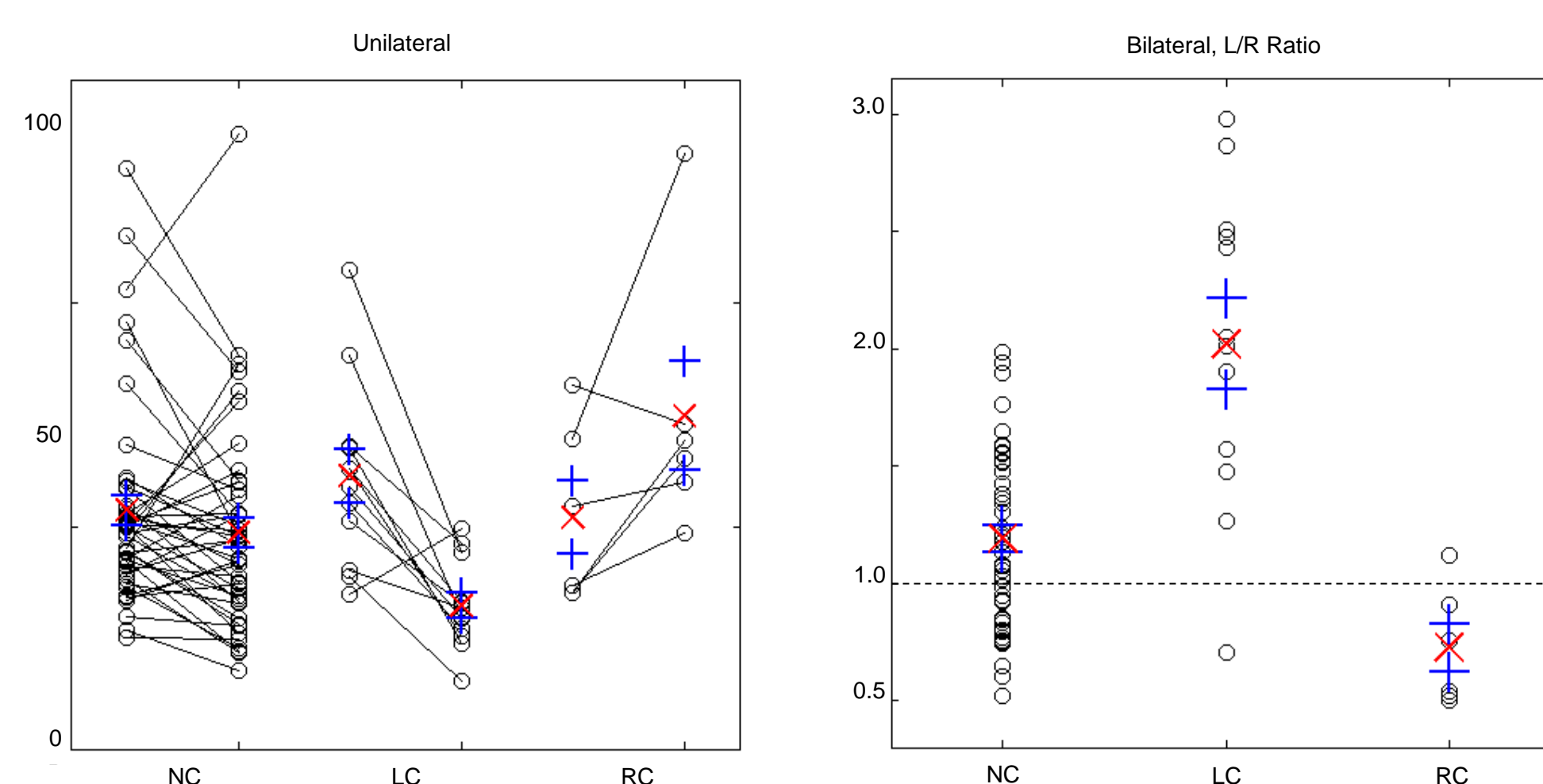


Figure 4. Individual-subject TSDSSD values derived from HbSat image time series. 'o' = individual-subject data values; 'x' = group mean value; '+' = mean ± SEM. The largest individual data value overall was arbitrarily set to 100, and all other values were rescaled in proportion.

Table 2. Representative ROC analysis results for the breast-cancer diagnosis problem.

Metric	LC vs. NC, 2 nd -Gen. Instrument, N _{Ca} = 12, N _{Non-Ca} = 45						RC vs. NC, 1 st -Gen. Instrument, N _{Ca} = 17, N _{Non-Ca} = 38					
	Hb	AUC (%)	Sens. (%)	Spec. (%)	# FPs	# FNs	Hb	AUC (%)	Sens. (%)	Spec. (%)	# FPs	# FNs
SMTSD	Sat	84.8	83.3	88.9	5	2	Oxy	77.4	70.6	81.6	7	5
	Sat	84.8	83.3	88.9	5	2	Deoxy	74.9	70.6	65.8	13	5
	Sat	84.8	83.3	88.9	5	2	Total	79.4	76.5	76.3	9	4
SSDTSD	Sat	85.7	83.3	91.1	4	2	Oxy	74.8	70.6	76.3	9	5
	Sat	85.4	83.3	88.9	5	2	Oxy	80.5	70.6	78.9	8	5

Results:

Inspection of the TSD spatial maps for women with unilateral breast cancer, as in the examples shown in Figure 2, reveals that this metric in most cases is larger in the tumor-bearing breast. The region of elevated SSD includes a large percentage of the breast volume, which extends well beyond the known structural borders of the tumor and is largely independent of the tumor's size. Corresponding results for women with benign breast lesions or with no known breast pathology do not show a comparable asymmetry.

When extended to group-level comparisons, all of the above-defined scalar metrics are seen to have larger values in the tumor-bearing breast, and little inter-breast disparity in subjects who do not have cancer (Figure 3). In unilateral comparisons, the left(right)-breast group mean metric value for women with left(right)-breast cancer is not significantly different from the left(right)-breast mean value for the non-cancer group. However, when bilateral comparisons are performed, by using the left-to-right breast ratio of metric values for all subjects (thereby minimizing inter-subject disparities that are unrelated to the presence or absence of cancer), there are highly significant group-mean differences between the non-cancer group and either breast-cancer group (Figure 4). As for the problem of predicting individual subjects' group membership (i.e., diagnosing breast-cancer): depending on the choice of hemodynamic parameter and scalar metric, ROC analysis [6] yields area-under-curve values in the range of 74-86%, sensitivities in the range of 70-84%, and specificities in the range of 76-92% (Table 2).

Discussion:

An important aspect of the performed image reconstruction, and subsequent analysis, is that they incorporate no prior knowledge of whether a subject has breast cancer or, for ones that do have it, of the tumor size or location, or even which is the tumor-bearing breast. Some might initially suppose that the minimal assumptions made account for the observation (see Figure 2) that the increased temporal standard deviation metric in the affected breast extends into regions far from the structural borders of the tumor. However, imaging results derived from fNIRS data collected during response to either applied-pressure or respiratory-gas maneuvers, which also did not make use of prior knowledge, have shown that tumor locations and sizes can be accurately extracted from those measurements ([7], and "Phenotype-Motivated Strategies for Optical Detection of Breast Cancer," this conference). Thus we conclude that resting-baseline recordings, processed in the manner presented here, are sensitive to dynamic vascular phenomena that do in fact extend over a large percentage of the breast volume.

A corollary that potentially has substantial clinical importance is that it may be possible to conduct breast-cancer screening by means of a simplified bilateral fNIRS measurement involving a small number of probes distributed over the surface of both breasts. Tests of a prototype device based on this hypothesis currently are under way.

References:

- [1] D. Hanahan and R.A. Weinberg, "The hallmarks of cancer," *Cell* **100**, 57-70 (2000).
- [2] D. Hanahan and R.A. Weinberg, "Hallmarks of cancer: The next generation," *Cell* **144**, 646-674 (2011).
- [3] R. Al abdi, H.L. Graber, Y. Xu, and R.L. Barbour, "Optomechanical imaging system for breast cancer detection," *J. Optical Society of America A* **28**, 2473-2493 (2011).
- [4] Y. Pei, H.L. Graber, and R.L. Barbour, "Influence of systematic errors in reference states on image quality and on stability of derived information for DC optical imaging," *Applied Optics* **40**, 5755-5769 (2001).
- [5] M.S. Lloyd and A.G. Nash, "Occult' breast cancer," *Annals of the Royal College of Surgeons of England* **83**, 420-424 (2001).
- [6] C.E. Metz, "Basic principles of ROC analysis," *Seminars in Nuclear Medicine* **8**, 283-298 (1978).
- [7] R. Al abdi, H.L. Graber, and R.L. Barbour, "Carbogen Inspiration Enhances Hemodynamic Contrast in the Cancerous Breast," Poster BSu3A.94 at Biomedical Optics and Digital Holography and Three-Dimensional Imaging (Miami, FL, April 29 - May 2, 2012).

Acknowledgements:

This research was supported by the National Institutes of Health (NIH) grant R41CA096102, the U.S. Army grant DAMD017-03-C-0018, the Susan G. Komen Foundation, the New York State Department of Health (Empire Clinical Research Investigator Program), the New York State Foundation for Science, Technology and Innovation-Technology Transfer Incentive Program (NYSTAR-TIPP) grant C020041, and NIRx Medical Technologies.